ARTICLE

Experimental Observables and Macroscopic Susceptibility/Microscopic Polarizability Tensors for Third and Fourth-Order Nonlinear Spectroscopy of Ordered Molecular System†

Yuan Wang[a], Zhi-feng Cui[a*], Hong-fei Wang[a,b*]

a. Department of Physics, Anhui Normal University, Wuhu 241000, China;
b. State Key Laboratory of Molecular Reaction Dynamics, Institute of Chemistry, Chinese Academy of Sciences, Beijing 100080, China

(Dated: Received on May 29, 2007; Accepted on June 20, 2007)

There has been emerging needs for the quantitative polarization analysis for the Coherent Anti-stokes Raman Spectroscopy and Coherent Anti-stokes Hyper-raman Spectroscopy, as the experimental studies with coherent anti-stokes raman spectroscopy and coherent anti-stokes hyper-raman spectroscopy for the interface and membrane studies being growing. Recently we have demonstrated that orientational analysis of linear and nonlinear spectroscopy from the ordered molecular system, such as molecular interfaces and films, can be carried out with the formulation of the orientational function in simple functional forms. Applications of such formulation for the second order spectroscopy, namely, the Second Harmonic Generation and Sum Frequency Generation Vibrational Spectroscopy, have helped to understand spectral and orientational details of the molecular interfaces and films. In order to employ this formulation for the higher order coherent nonlinear spectroscopy, the detailed expressions of the experimental observables and the macroscopic susceptibility/microscopic polarizability tensors for the third and fourth-order nonlinear spectroscopy for the interface or film is presented with the rotational symmetry. General expressions for the typical third and fourth order spectroscopy, such as the Third Harmonic Generation, the degenerated coherent anti-stokes raman spectroscopy, the Fourth Harmonic Generation and the degenerated coherent anti-stokes hyper-raman spectroscopy, are presented for their future applications. The advantages and limitations of the third and fourth order spectroscopic techniques are also discussed.

Key words: Third and fourth-order nonlinear spectroscopy, Experimental observable, Macroscopic susceptibility/microscopic polarizability tensor, Ordered molecular system

I. INTRODUCTION

Ordered or aligned molecular systems, such as interfaces, organic films and biological membranes, are not only fundamentally interesting but also technologically important [1-5]. Spectroscopy with polarized light is the ultimate tool for studying ordered molecular systems, because in principle very useful molecular information, including the knowledge on molecular ordering, i.e., orientation and orientational distribution, and the knowledge on molecular structure and conformation, can be obtained from the measurement of the molecular responses to the polarized light [6].

However, the task in carrying out the designed measurement and making interpretation from the measured data is not always simple or easy, even though tremendous advances has been made in understanding the ordered molecular systems through various spectroscopic tools. For example, the second order nonlinear spectroscopic techniques, i.e. Second Harmonic Generation (SHG) and Sum Frequency Generation Vibrational Spectroscopy (SFG-VS) have been developed in the past two decades in interface studies for their unique interface specificity and submonolayer sensitivity [7,8]. However, better quantitative understanding of the spectroscopy and orientational order of the molecular interface using SHG and SFG-VS is still an ongoing effort and outgrowing field [9-11]. Such quantitative understanding is built on the understanding of the coherent and polarization dependent nature of the SHG and SFG-VS processes, as well as the understanding of the symmetry of the molecular hyperpolarizability tensors. Together they enable the explicit connections between the experimental observables in SHG and SFG-VS directly to the macroscopic susceptibility and microscopic (molecular) polarizability tensors [5,9-13]. Particularly, the introduction of the general orientational functional formulation in SHG and SFG-VS brought a relatively simple frame to understand the rather complicated dependence of the SHG and SFG-VS response to the various variables, such as the polarization, experimental configuration, molecular orientation, and molecular symmetry, etc [5,9,10,14]. This development also led to the development of very useful tools in the SHG and SFG-VS studies, such as the polarization selection rules

†Part of the special issue "Cun-hao Zhang Festschrift".
*Authors to whom correspondence should be addressed. E-mail: hongfei@iccas.ac.cn, Tel.: +86-10-62555347, Fax: +86-10-62563167, E-mail: zfcui@mail.ahnu.edu.cn, Tel: +86-553-3869748, Fax: +86-553-3869748

in assignment of vibrational spectral peaks in SFG-VS [15,16], the polarization null angle (PNA) method for accurate measurement of orientational parameters of molecular groups [17,18], the experimental configuration analysis for understanding the detailed spectral interference between different spectral features [19,20], etc., and this also led to novel and detailed understanding of the spectroscopy and orientational structure of quite a few important and benchmark liquid interfaces, such as the air/methanol, air/ethanol, and air/water interfaces [20-26].

Higher-order nonlinear spectroscopic techniques, such as the third order Coherent Anti-Stokes Raman Spectroscopy (CARS) [27-34] and the fourth order Coherent Anti-Stokes Hyper-Raman Spectroscopy (CAHRS)[1] [35-39], have been recently employed to investigate or image molecular interfaces and biological membranes. Being Raman spectroscopy, the clear advantage of the CARS and the CAHRS is that they do not directly use the infrared laser pulses that generally have trouble to penetrate the condensed phase as in the ordinary IR or SFG vibrational spectroscopy, for obtaining the coherent molecular vibrational spectra of the buried interfaces and membranes. The fourth order CAHRS process is particularly interesting because it is also an interface specific process just as the SFG-VS [35-39]. However, the fourth order CAHRS is expected to be two or more orders weaker than the second order SFG-VS processes. So far the CAHRS from the liquid interfaces was only observed with the help of the electronic resonance enhancement from the interfacial molecules [35-39], and more efficient detection of the weaker electronically non-resonant CAHRS is yet to be developed.

However, as in the SHG and SFG-VS [9,10], the ability for both the CARS and the CAHRS to investigate the molecular detail of the interface and membrane molecules lies on our ability to make accurate measurements on the experimental observables in the CARS or CAHRS processes, and also lies on our ability to understand the specific connections between these observables and the macroscopic susceptibility/microscopic polarizability tensors of the ordered molecular interfaces or membranes. The latter two processes are obviously more complicated than the second order SHG and SFG-VS processes, because for the higher order processes, higher order rank tensors, i.e. exponentially increasing number of tensor elements, are generally involved. Therefore, in order to be able to obtain quantitative molecular information from the CARS and CAHRS data, what has been developed for the SHG and SFG-VS also has to be done for the CARS and CAHRS [9-13,42,43].

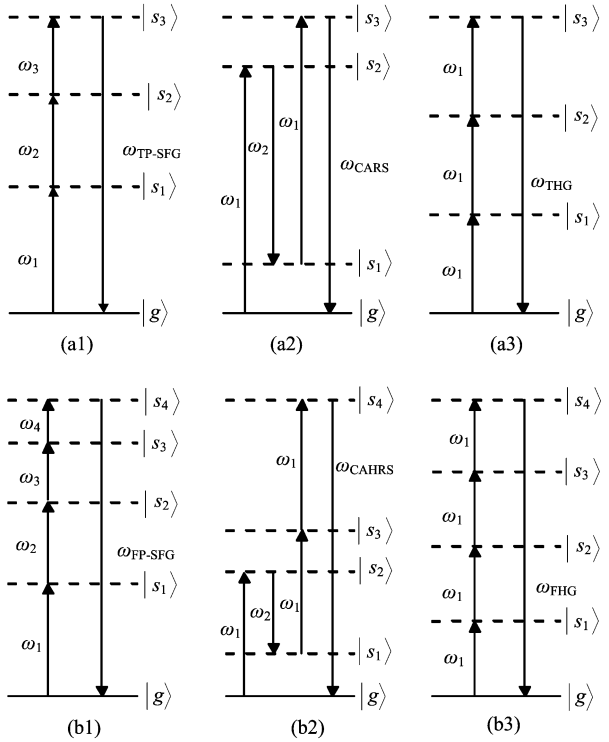

FIG. 1 Schematic transitions for third-order and fourth-order nonlinear effects: (a1) the general Three Photon Sum Frequency Generation (TP-SFG), i.e. $\omega = \omega_1+\omega_2+\omega_3$; (a2) CARS, i.e. $\omega = 2\omega_1 - \omega_2$; (a3) Third Harmonic Generation (THG), i.e. $\omega = 3\omega_1$; (b1) the general Four Photon Sum Frequency Generation (FP-SFG), i.e. $\omega = \omega_1+\omega_2+\omega_3+\omega_4$; (b2) CAHRS, i.e. $\omega = 3\omega_1 - \omega_2$; (b3) Fourth Harmonic Generation (FHG), i.e. $\omega = 4\omega_1$; respectively. $|g\rangle$, $|s_1\rangle$, $|s_2\rangle$, $|s_3\rangle$, and $|s_4\rangle$ represent the ground state and the virtual (real for the electronically resonant case) upper energy levels, respectively. For the CARS (a2) and the CAHRS (b2) processes, the $|s_1\rangle$ level represents the vibrational state.

In a recent work, one of the authors formulated a simplified general formulation of the orientational functional, i.e. $R(\theta)$ with θ as the tilted angle of the symmetry axis from the interface normal, of the linear and nonlinear spectroscopy for the ordered molecular system [5]. With this formulation, the orientational response of the spectroscopic intensity in different experimental configurations of the ordered molecular system can be well described with the different behaviors of the $R(\theta)$ [9,10,14]. The derivation of the coefficients, or the general orientational parameters in each $R(\theta)$, can only be obtained with the knowledge of the ex-

[1] Here we need to clarify the terminology of CARS and CAHRS. The CARS process, as shown in Fig.1 (a2), is a process with a Stokes Raman plus an anti-Stokes Raman. Here the fourth-order CAHRS, as shown in Fig.1 (b2), is a Stokes Raman plus an anti-Stokes Hyper Raman. However, in Ref.[40,41], the process of a Stokes Hyper Raman plus an anti-Stokes Hyper Raman ($4\omega_1-\omega_2$) was called the coherent hyper-Raman scattering (CHRS) or the CAHRS. In order to avoid confusion, we suggest to call the CAHRS in this work as the fourth-order CAHRS, and to call the CHRS or CAHRS in those two references as the fifth-order CAHRS. In this work, CAHRS is used for the fourth-order CAHRS unless specified otherwise.

DOI:10.1088/1674-0068/20/04/449-460

perimental observables and the macroscopic susceptibility/microscopic polarizability tensors of the ordered molecular interfaces or membranes, and the examples for SHG and SFG-VS can be found in the recent literature [9,10,14,16]. Particularly, Hirose *et al.* gave a complete list of all the possible expressions for the SFG-VS process [13]. As the development of the experiments with the CARS and the CAHRS vibrational spectroscopy for interface and membrane studies, there are emerging needs for the quantitative polarization analysis of the CARS and CAHRS processes [29-31,34-39]. Therefore, in order to do the same for the third and fourth order spectroscopy, the job in this report is to describe the relationships of the experimental observables and the macroscopic susceptibility/microscopic polarizability tensors of the ordered molecular interfaces or membranes in the CARS and CAHRS, as well as the Third Harmonic Generation (THG) and Fourth Harmonic Generation (FHG) processes for further applications of these techniques.

In this report, we shall first discuss the general formulation of the $R(\theta)$ for the third and fourth order coherent spectroscopy. Then we shall summarize the results of the connections between the experimental observables and the macroscopic susceptibility/microscopic polarizability tensors for the third order and fourth order coherent spectroscopy, especially for the CARS, THG, CAHRS and FHG processes in the desirable experimental configurations in the reflective geometry. These results can explicitly lead to the calculation of the general orientational parameters in the $R(\theta)$s for these coherent optical processes. The discussion of the further simplification with the bond polarizability derivative model and its empirical calculation for the CARS and CAHRS vibrational spectroscopy will be discussed elsewhere.

II. FORMULATION OF ORIENTATIONAL FUNCTIONAL

A. Definition and experimental implications of $R_n(\theta)$

Here we briefly discuss the usefulness of the formulation of the orientational functional and how it is connected to the experimental observables in the coherent nonlinear spectroscopy.

Molecules are generally ordered at the interface, in a film or in a membrane. In description of the orientational order of a molecular system, the orientational angles (θ,ϕ,ψ) and the orientational distribution function ($f(\theta,\phi,\psi)$) are required. In practice, the orientational distribution function of the ensemble of the ordered molecular system can be described by the moments of a certain polynomial function. For example, when only the tilt angle θ is important, the orientational distribution function is

$$f(\theta) = \frac{1}{A}\sum_{n=0}^{\infty}\left(\frac{2n+1}{2}\right)\langle\cos^n\theta\rangle\cos^n\theta = \frac{1}{A}\sum_{n=0}^{\infty}\left(\frac{2n+1}{2}\right)\langle P_n\rangle P_n \quad (1)$$

in which n is integer from 0 to ∞, and A is the normalization factor $A=\int_0^{\pi} f(\theta)\sin\theta\mathrm{d}\theta$. $\cos^n\theta$ and P_n are the nth order moment of the trigonometric series or the Legendre polynomial series of $\cos\theta$ as the variable, respectively. Their ensemble averages over the whole molecular system, i.e. $\langle\cos^n\theta\rangle$ and $\langle P_n\rangle$, are defined as below [44].

$$\langle\cos^n\theta\rangle = \int_0^{\pi} f(\theta)\cos^n\theta\sin\theta\mathrm{d}\theta \quad (2)$$

$$\langle P_n\rangle = \int_0^{\pi} f(\theta)P_n\sin\theta\mathrm{d}\theta \quad (3)$$

here we see that the trigonometric series or the Legendre polynomial series are equivalent in description of the $f(\theta)$, and the transformation between these two series is linear. The orientational factor in the product of two vectors is simply $\cos\theta$. Therefore, the higher order interaction between the molecular dipole and the electric field vectors is described with the $\cos^n\theta$ series or their mathematical equivalent. As we have shown recently [5], the orientational functional of the nth order coherent nonlinear spectroscopy is

$$R_n(\theta) = \left|\sum_{j}^{n+1,n-1,n-3,\ldots} c_j^{(n)}\langle\cos^j\theta\rangle\right|^2 \quad (4)$$

and the orientational dependent intensity is

$$I_n \propto \left|\chi_{\mathrm{eff}}^{(n)}\right|^2 = N^2\times {d_n}^2\times R_n(\theta) \quad (5)$$

Here $j\geq 0$ and $c_j^{(n)}$ is a unitless number and is called the jth general orientational parameter. N is the number of molecules of the molecular system, and d_n is the orientational independent intensity factor, which bears the same unit as $\beta_{i'j'k'l'\ldots}$. Therefore, for the second, third and fourth order coherent nonlinear spectroscopy of a ordered molecular system, their $R_n(\theta)$ are as follows:

$$\begin{aligned} R_2(\theta) &= \left|\langle\cos\theta\rangle + c_3^{(2)}\langle\cos^3\theta\rangle\right|^2 \\ R_3(\theta) &= \left|1 + c_2^{(3)}\langle\cos^2\theta\rangle + c_4^{(3)}\langle\cos^4\theta\rangle\right|^2 \\ R_4(\theta) &= \left|\langle\cos\theta\rangle + c_3^{(4)}\langle\cos^3\theta\rangle + c_5^{(4)}\langle\cos^5\theta\rangle\right|^2 \end{aligned} \quad (6)$$

In general, the higher order optical process probes both the higher order of $\langle\cos^n\theta\rangle$s as well as the lower

DOI:10.1088/1674-0068/20/04/449-460

order of $\langle\cos^n\theta\rangle$s. Therefore, the behavior of higher order $R_n(\theta)$ is much more complicated, which is somehow an unpleasant fact, but on the other hand higher order $R_n(\theta)$ provides much more sensitive measurement of the molecular orientation in the ordered molecular system. The formulation of the $R_n(\theta)$ has provided a general framework for sensitive orientational analysis with nonlinear spectroscopy [5,14].

These expressions for these $R_n(\theta)$s have direct implications in the experiment studies. From Eq.(4) and Eq.(6) one can clearly see the difference between the odd and even order nonlinear processes. For the even order processes, their $R_n(\theta)$s are purely orientational dependent, i.e. j=2m+1 is odd and all the terms are function with odd order $\cos^{2m+1}\theta$ (m=0,...,n/2)s; while for the odd order processes, their $R_n(\theta)$s are not purely orientational dependent, i.e. j=2m is even and when m=0 for the even order process $\cos^{2m}\theta$ (m=0,...,(n+1)/2) term becomes a constant 1. This indicates that in general the odd order process is not as orientational sensitive as the even order optical processes. For example, in $R_3(\theta)$ in Eq.(6), unless $c_2^{(3)}$ and $c_4^{(3)}$ are large numbers, $R_3(\theta)$ is going to be dominated by the first term 1, the non-orientational dependent. The general existence of the orientational independent contributions in the third order processes explains why there are generally significant orientational independent background signal in the third order CARS imaging experiment [29-33]. On the other hand, this is an advantage in CARS imaging since when there is low level background CARS signal, one can conclude that there is little population of the species which may contribute to the CARS signal. In contrast, the even order processes is much more sensitive to the orientation changes in the ordered molecular system. This advantage for orientational analysis has been well demonstrated with the recent successes in SFG-VS and SHG, which are the second order processes [9,10,14,18-21,25,26]. This also assures the possibility of better contrast ratio in SFG-VS and SHG imaging than that of CARS imaging [45,46].

B. Derivation of $R_n(\theta)$

From Eq.(5), one can see that the simplified expression $N^2\times d_n^2\times R_n(\theta)$ is directly derived from the term $\chi_{\rm eff}^{(n)}$, which is the effective nth order nonlinear susceptibility of the molecular system in response to the optical field. The expression for $\chi_{\rm eff}^{(n)}$ is quite complicated, because it involves the experimental configuration, polarization, local field factors, and the macroscopic susceptibility/microscopic polarizability tensors, etc. However, the simplified expression $N^2\times {d_n}^2\times R_n(\theta)$ in different experimental configuration and polarization makes it physically clear to perform quantitative spectral symmetry and orientational analysis of the ordered molecular systems. The usefulness of such formulation has been well demonstrated in the recent SHG and SFG-VS studies of the molecular interfaces [9,10,14-16,18-21,25,26]. This was possible because the experimental observables and their connection to the macroscopic susceptibility/microscopic polarizability tensors were thoroughly studied and formulated, so the d and c parameters in SHG and SFG-VS in each different cases can be readily worked out and used for quantitative analysis of the experimental data [9,10,19-21].

Such connections are based on the following two relationships, namely, the connection between the $\chi_{\rm eff}^{(n)}$ and the macroscopic susceptibility tensors $\chi_{ijkl\ldots}^{(n)}$, and the connection between the $\chi_{ijkl\ldots}^{(n)}$ tensors and the microscopic polarizability tensors $\beta_{i'j'k'l'\ldots}^{(n)}$. The first connection does not involve the detailed molecular properties and the only second connection requires the knowledge of the molecular symmetry as well as the knowledge of the molecular orientation and orientational distribution. Nevertheless, as one can easily see, because the number of tensors increases exponentially as the order goes higher, such relationships become much more complicated accordingly. We have the followings [5]:

$$\begin{aligned}\chi_{\rm eff}^{(n)} &= [L(\omega)\cdot\vec{e}_\omega]\cdot\chi^{(n)}:[L(\omega_1)\cdot\vec{e}_{\omega_1}]\,[L(\omega_2)\cdot\vec{e}_{\omega_2}]\\ &\quad\cdot[L(\omega_3)\cdot\vec{e}_{\omega_3}]\cdots\\ &= \sum_{i,j,k,l,\ldots}\chi_{ijkl\ldots}^{(n)}\times\{[L(\omega)\cdot\vec{e}_\omega]_i\,[L(\omega_1)\cdot\vec{e}_{\omega_1}]_j\\ &\quad\cdot[L(\omega_2)\cdot\vec{e}_{\omega_2}]_k\,[L(\omega_3)\cdot\vec{e}_{\omega_3}]_l\cdots\} \qquad (7)\end{aligned}$$

$$\chi_{ijkl}^{(n)} = N\times\sum_{\substack{i',j',k',l',\ldots\\=a,b,c}}\langle R_{ii'}R_{jj'}R_{kk'}R_{ll'}\ldots\rangle\beta_{i'j'k'l'\ldots}^{(n)} \qquad (8)$$

here the ω_is (i=1,...n) are the frequencies of the optical fields involved in the nth nonlinear process, and ω is the frequency of the optical signal, i.e. $\omega=\omega_1\pm\omega_2\pm\omega_3\pm\cdots$. $\vec{e}_{\omega_i}$ is the unit vector of the optical field with ω_i, and the $L(\omega_i)$ is the tensorial Fresnel factor [9]. The indexes i,j,k,l... and i',j',k',l'... each represent the three possible coordinates in the laboratory (x,y,z) and the molecular (a,b,c) coordinates, respectively, and $R_{ii'}$s are the matrix elements of the Euler transformation matrix from the molecular coordinates to the laboratory coordinates [5,47].

The orientational ensemble average in Eq.(8) is defined as

$$\begin{aligned}&\langle R_{ii'}R_{jj'}R_{kk'}R_{ll'}\cdots\rangle\\ &\quad=\frac{\int(R_{ii'}R_{jj'}R_{kk'}R_{ll'}\cdots)\times e^{-U(\theta,\phi,\psi)/kT}\mathrm{d}\Omega}{\int e^{-U(\theta,\phi,\psi)/kT}\mathrm{d}\Omega} \qquad (9)\end{aligned}$$

where $U(\theta,\phi,\psi)$ is the potential energy associated with different molecular orientation angles (θ,ϕ,ψ), and

DOI:10.1088/1674-0068/20/04/449-460

$f(\theta,\phi,\psi) = e^{-U(\theta,\phi,\psi)/kT}$. k in the exponential is the Boltzmann constant, T is the system temperature, and $\mathrm{d}\Omega = \sin\theta \mathrm{d}\theta\mathrm{d}\phi\mathrm{d}\psi$ is the differential element of the solid angle $\Omega(\theta,\phi,\psi)$. Usually in an ordered molecular system the Euler angle θ, which is the angle between the molecular main axis c and the laboratory z axis, and its distribution are interested. For most of the ordered molecular systems, rotational isotropy would make the potential energy $U(\theta,\phi,\psi)$=$U(\theta)$, or in some cases $U(\theta,\phi,\psi)$=$U(\theta,\psi)$. In the case of $U(\theta,\phi,\psi)$=$U(\theta)$, the integration over ϕ and ψ would be separable from the θ terms.

The difficulty in quantitative orientational analysis in higher order nonlinear spectroscopy is obvious. There are 3^{n+1} possible tensor elements for both the $\chi^{(n)}_{ijkl\ldots}$ and $\beta^{(n)}_{i'j'k'l'\ldots}$, e.g. 81 for the third order and 243 for the fourth order. Even though with the consideration of symmetry, both numbers of the non-zero elements for $\chi^{(n)}_{ijkl\ldots}$ and $\beta^{(n)}_{i'j'k'l'\ldots}$ can be significantly reduced, which shall be discussed in the next sections, it is still a formidable task to relate many $\chi^{(n)}_{ijkl\ldots}$ tensors through the angular dependent tensor production to the $\chi^{(n)}_{\mathrm{eff}}$, as well as to express the many $\chi^{(n)}_{ijkl\ldots}$ tensors through the orientational ensemble average to the as many $\beta^{(n)}_{i'j'k'l'\ldots}$ tensors.

Therefore, in order to simplify and make quantitative orientational and spectral analysis with the third and fourth order coherent nonlinear spectroscopies for ordered molecular systems with the rotational symmetry ($C_{\infty v}$), in the next sections, we shall derive the explicit relationships between the experimental observables and the macroscopic susceptibility/microscopic polarizability tensors for some of the more generally used third and fourth order processes. The experimentally independent measurable terms for each process shall be listed, and their explicit expressions with the corresponding non-zero $\chi^{(n)}_{ijkl\ldots}$ and $\beta^{(n)}_{i'j'k'l'\ldots}$ tensors shall be given. Besides the formulas, issues and concerns in the experimental measurement shall also be discussed.

III. THIRD-ORDER NONLINEAR SPECTROSCOPY: THG AND CARS

The third-order nonlinear spectroscopy is usually called the four-wave-mixing spectroscopy (Four-WMS) [48]. The general Three Photon Sum Frequency Generation (TP-SFG) and two typical Four-WMS processes, i.e. THG and CARS, are illustrated in Fig.1(a).

A. general experimental observables in Four-WMS processes

According to Eq.(7), the general expression of $\chi^{(3)}_{\mathrm{eff}}$ for the third order process is

$$\chi^{(3)}_{\mathrm{eff}} = \sum_{i,j,k,l} \chi^{(3)}_{ijkl} \times \{[L(\omega)\cdot\vec{e}_{\omega}]_i [L(\omega_1)\cdot\vec{e}_{\omega_1}]_j \cdot [L(\omega_2)\cdot\vec{e}_{\omega_2}]_k [L(\omega_3)\cdot\vec{e}_{\omega_3}]_l\} \quad (10)$$

When the surface or the film is achiral and rotationally isotropic respect to the surface normal, i.e. with the $C_{\infty v}$ symmetry, the 81 $\chi^{(3)}_{ijkl}$ tensor terms are simplified into the following non-vanishing tensor element terms. In this case, there are 21 non-vanishing and 10 independent macroscopic tensor elements as the followings [49]. A detailed tutorial on how to derive these tensor terms in different symmetry for SFG-VS can be found in the literature [50]. The derivation for the third order terms is similar.

$$\begin{aligned}
&\chi^{(3)}_{xxyy} = \chi^{(3)}_{yyxx}, \chi^{(3)}_{xyxy} = \chi^{(3)}_{yxyx}, \chi^{(3)}_{xyyx} = \chi^{(3)}_{yxxy}\\
&\chi^{(3)}_{zzxx} = \chi^{(3)}_{zzyy}, \chi^{(3)}_{zxzx} = \chi^{(3)}_{zyzy}, \chi^{(3)}_{xzzx} = \chi^{(3)}_{yzzy}\\
&\chi^{(3)}_{xxzz} = \chi^{(3)}_{yyzz}, \chi^{(3)}_{xzxz} = \chi^{(3)}_{yzyz}, \chi^{(3)}_{zxxz} = \chi^{(3)}_{zyyz}\\
&\chi^{(3)}_{xxxx} = \chi^{(3)}_{yyyy}, \chi^{(3)}_{zzzz}
\end{aligned} \quad (11)$$

and with the relationship

$$\chi^{(3)}_{xxxx} = \chi^{(3)}_{xxyy} + \chi^{(3)}_{xyxy} + \chi^{(3)}_{xyyx} \quad (12)$$

The simplest case in the orientational analysis is to make all the beam coplanar and the signal is in the direction of reflection. When all three incoming optical beams are in different incident angle and polarization, for a rotationally symmetric molecular system ($C_{\infty v}$), there are only 8 experimentally independent terms. The expression for an arbitrary $\chi^{(3)}_{\mathrm{eff,TP-SFG}}$ in terms of these independent observables is

$$\begin{aligned}
\chi^{(3)}_{\mathrm{eff,TP-SFG}} = {} & \cos\alpha\cos\alpha_1\cos\alpha_2\cos\alpha_3\chi^{(3)}_{\mathrm{eff},pppp}\\
&+ \sin\alpha\sin\alpha_1\sin\alpha_2\sin\alpha_3\chi^{(3)}_{\mathrm{eff},ssss}\\
&+ \cos\alpha\sin\alpha_1\sin\alpha_2\cos\alpha_3\chi^{(3)}_{\mathrm{eff},pssp}\\
&+ \sin\alpha\cos\alpha_1\cos\alpha_2\sin\alpha_3\chi^{(3)}_{\mathrm{eff},spps}\\
&+ \cos\alpha\cos\alpha_1\sin\alpha_2\sin\alpha_3\chi^{(3)}_{\mathrm{eff},ppss}\\
&+ \cos\alpha\sin\alpha_1\cos\alpha_2\sin\alpha_3\chi^{(3)}_{\mathrm{eff},psps}\\
&+ \sin\alpha\sin\alpha_1\cos\alpha_2\cos\alpha_3\chi^{(3)}_{\mathrm{eff},sspp}\\
&+ \sin\alpha\cos\alpha_1\sin\alpha_2\cos\alpha_3\chi^{(3)}_{\mathrm{eff},spsp}
\end{aligned} \quad (13)$$

in which s and p are the optical field polarization perpendicular and parallel to the incident plane, respectively. The four number index represents the polarizations of the fields following the order of ω, ω_1, ω_2, and ω_3, respectively. The α and α_i represent the polarization angles from the incident plane of the corresponding electric fields, respectively. We have

$$\chi^{(3)}_{\mathrm{eff},pppp} = \chi^{(3)}_{zzzz} L_{zz}(\omega) L_{zz}(\omega_1) L_{zz}(\omega_2) L_{zz}(\omega_3) \cdot \sin\Omega\sin\Omega_1\sin\Omega_2\sin\Omega_3$$

DOI:10.1088/1674-0068/20/04/449-460

$$
\begin{aligned}
&+\chi^{(3)}_{zxxz}L_{zz}(\omega)L_{xx}(\omega_1)L_{xx}(\omega_2)L_{zz}(\omega_3)\\
&\cdot\sin\Omega\cos\Omega_1\cos\Omega_2\sin\Omega_3\\
&\mp\chi^{(3)}_{xxxx}L_{xx}(\omega)L_{xx}(\omega_1)L_{xx}(\omega_2)L_{xx}(\omega_3)\\
&\cdot\cos\Omega\cos\Omega_1\cos\Omega_2\cos\Omega_3\\
&\mp\chi^{(3)}_{xzzx}L_{xx}(\omega)L_{zz}(\omega_1)L_{zz}(\omega_2)L_{xx}(\omega_3)\\
&\cdot\cos\Omega\sin\Omega_1\sin\Omega_2\cos\Omega_3\\
&\pm\chi^{(3)}_{zzxx}L_{zz}(\omega)L_{zz}(\omega_1)L_{xx}(\omega_1)L_{xx}(\omega_3)\\
&\cdot\sin\Omega\sin\Omega_1\cos\Omega_2\cos\Omega_3\\
&\pm\chi^{(3)}_{zxzx}L_{zz}(\omega)L_{xx}(\omega_1)L_{zz}(\omega_1)L_{xx}(\omega_3)\\
&\cdot\sin\Omega\cos\Omega_1\sin\Omega_2\cos\Omega_3\\
&-\chi^{(3)}_{xxzz}L_{xx}(\omega)L_{xx}(\omega_1)L_{zz}(\omega_2)L_{zz}(\omega_3)\\
&\cdot\cos\Omega\cos\Omega_1\sin\Omega_2\sin\Omega_3\\
&-\chi^{(3)}_{xzxz}L_{xx}(\omega)L_{zz}(\omega_1)L_{xx}(\omega_2)L_{zz}(\omega_3)\\
&\cdot\cos\Omega\sin\Omega_1\cos\Omega_2\sin\Omega_3 \qquad (14)
\end{aligned}
$$

$$\chi^{(3)}_{\mathrm{eff},ssss}=\pm\chi^{(3)}_{yyyy}L_{yy}(\omega)L_{yy}(\omega_1)L_{yy}(\omega_2)L_{yy}(\omega_3) \qquad (15)$$

$$
\begin{aligned}
\chi^{(3)}_{\mathrm{eff},pssp}&=\chi^{(3)}_{zyyz}L_{zz}(\omega)L_{yy}(\omega_1)L_{yy}(\omega_2)L_{zz}(\omega_3)\\
&\cdot\sin\Omega\sin\Omega_3\mp\chi^{(3)}_{xyyx}L_{xx}(\omega)L_{yy}(\omega_1)\\
&\cdot L_{yy}(\omega_2)L_{xx}(\omega_3)\cos\Omega\cos\Omega_3 \qquad (16)\\
\chi^{(3)}_{\mathrm{eff},spps}&=\pm\chi^{(3)}_{yzzy}L_{yy}(\omega)L_{zz}(\omega_1)L_{zz}(\omega_2)L_{yy}(\omega_3)\\
&\cdot\sin\Omega_1\sin\Omega_2\pm\chi^{(3)}_{yxxy}L_{yy}(\omega)L_{xx}(\omega_1)\\
&\cdot L_{xx}(\omega_2)L_{yy}(\omega_3)\cos\Omega_1\cos\Omega_2 \qquad (17)\\
\chi^{(3)}_{\mathrm{eff},ppss}&=\pm\chi^{(3)}_{zzyy}L_{zz}(\omega)L_{zz}(\omega_1)L_{yy}(\omega_2)L_{yy}(\omega_3)\\
&\cdot\sin\Omega\sin\Omega_1\mp\chi^{(3)}_{xxyy}L_{xx}(\omega)L_{xx}(\omega_1)\\
&\cdot L_{yy}(\omega_2)L_{yy}(\omega_3)\cos\Omega\cos\Omega_1 \qquad (18)\\
\chi^{(3)}_{\mathrm{eff},psps}&=\pm\chi^{(3)}_{zyzy}L_{zz}(\omega)L_{yy}(\omega_1)L_{zz}(\omega_2)L_{yy}(\omega_3)\\
&\cdot\sin\Omega\sin\Omega_2\mp\chi^{(3)}_{xyxy}L_{xx}(\omega)L_{yy}(\omega_1)\\
&\cdot L_{xx}(\omega_2)L_{yy}(\omega_3)\cos\Omega\cos\Omega_2 \qquad (19)\\
\chi^{(3)}_{\mathrm{eff},sspp}&=\pm\chi^{(3)}_{yyzz}L_{yy}(\omega)L_{yy}(\omega_1)L_{zz}(\omega_2)L_{zz}(\omega_3)\\
&\cdot\sin\Omega_2\sin\Omega_3+\chi^{(3)}_{yyxx}L_{yy}(\omega)L_{yy}(\omega_1)\\
&\cdot L_{xx}(\omega_2)L_{xx}(\omega_3)\cos\Omega_2\cos\Omega_3 \qquad (20)\\
\chi^{(3)}_{\mathrm{eff},spsp}&=\pm\chi^{(3)}_{yzyz}L_{yy}(\omega)L_{zz}(\omega_1)L_{yy}(\omega_2)L_{zz}(\omega_3)\\
&\cdot\sin\Omega_1\sin\Omega_3+\chi^{(3)}_{yxyx}L_{yy}(\omega)L_{xx}(\omega_1)\\
&\cdot L_{yy}(\omega_2)L_{xx}(\omega_3)\cos\Omega_1\cos\Omega_3 \qquad (21)
\end{aligned}
$$

here the upper or lower signs represent the co-propagation with the three incident beams in the same quadrant or the counter-propagation with the three incident beams in two different quadrants configurations as illustrated in Fig.2, respectively. In deriving above equations, the following unit optical field vectors are used.

$$\vec{e_\omega}=\begin{pmatrix}-\cos\alpha\cos\Omega\\-\sin\alpha\\\cos\alpha\sin\Omega\end{pmatrix} \qquad (22)$$

$$\vec{e_{\omega_1}}=\begin{pmatrix}\cos\alpha_1\cos\Omega_1\\-\sin\alpha_1\\\cos\alpha_1\sin\Omega_1\end{pmatrix} \qquad (23)$$

$$\vec{e_{\omega_2}}=\begin{pmatrix}\cos\alpha_2\cos\Omega_2\\-\sin\alpha_2\\\cos\alpha_2\sin\Omega_2\end{pmatrix} \qquad (24)$$

$$\vec{e_{\omega_3}}=\begin{pmatrix}\cos\alpha_3\cos\Omega_3\\-\sin\alpha_3\\\cos\alpha_3\sin\Omega_3\end{pmatrix}_{\mathrm{co-propagation}} \qquad (25)$$

$$\text{or}\quad\begin{pmatrix}-\cos\alpha_3\cos\Omega_3\\\sin\alpha_3\\\cos\alpha_3\sin\Omega_3\end{pmatrix}_{\mathrm{counter-propagation}} \qquad (26)$$

Since there are 10 independent non-vanishing $\chi^{(3)}_{ijkl}$ elements, the 8 independent measurement can not give the information of each $\chi^{(3)}_{ijkl}$ elements. This is the intrinsic problem for the nonlinear optical measurements, unless further reduction of the number of the independent non-vanishing $\chi^{(3)}_{ijkl}$ elements can be made. In the degenerated cases such as CARS or THG, the number of the independent measurements as well as the number independent non-vanishing $\chi^{(3)}_{ijkl}$ and $\beta^{(3)}_{i'j'k'l'}$ elements are expected to be reduced. One exception is that in the CARS vibrational spectroscopy ($\omega=2\omega_1-\omega_2$, with $\omega_1-\omega_2=\omega_{\mathrm{vib}}$), the number of independent $\beta^{(3)}_{i'j'k'l'}$ elements can not be reduced, because $\beta^{(3)}_{i'j'k'l'}\neq\beta^{(3)}_{i'k'j'l'}$ when $j'\neq k'$, even though both these two correspond to the same frequency ω_1. However, in this case, $\beta^{(3)}_{i'j'k'l'}$ and $\beta^{(3)}_{i'k'j'l'}$ have to belong to either the symmetric or the asymmetric vibrational mode, respectively, and they have to be treated separately. Thus, the actual number of the terms in each treatment is also reduced. In general, the analysis for CARS and THG becomes much simpler. The details of all these terms for CARS and THG are listed in the supplementary materials for this paper.

B. The experimental configuration for the CARS

Once the incident angles (Ω_1,Ω_2,Ω_3) of the three incoming beam is fixed coplanar, the angle of the outgoing signal Ω is also fixed with

$$\sin\Omega=\frac{|\vec{k}_1|\sin\Omega_1+|\vec{k}_2|\sin\Omega_2\mp|\vec{k}_3|\sin\Omega_3}{|\vec{k}|} \qquad (27)$$

here, $\vec{k}_i$ is the wave vector of beam of ω_i in the direction of the corresponding beam propagation. The upper and

DOI:10.1088/1674-0068/20/04/449-460

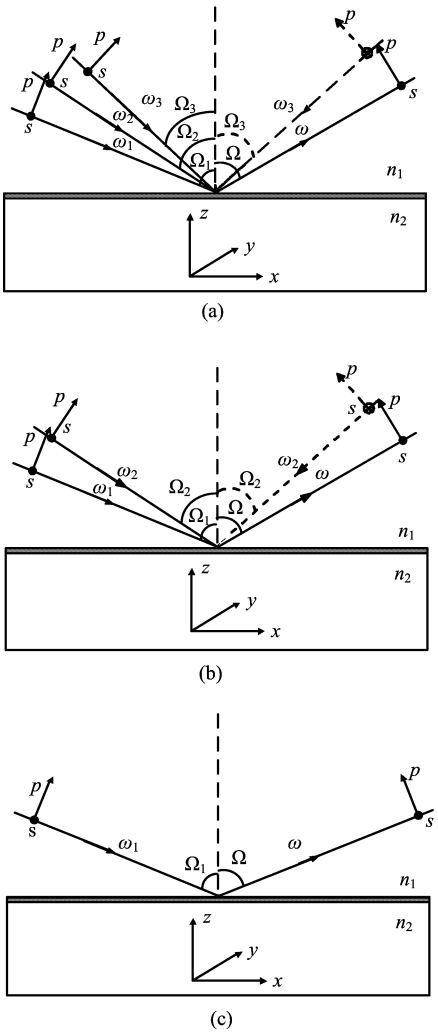

FIG. 2 Geometry of interfacial (a) TP-SFG, (b) CARS, and (c) THG in the laboratory coordinate system. In (a) and (b), the dotted lines represent the counter-propagation configuration, while the solid line represents the co-propagation geometry.

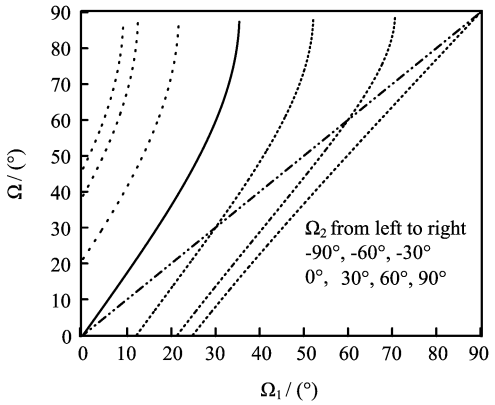

FIG. 3 The possible output angle Ω as a function of the incident angle Ω_1 for the reflective CARS experimental configuration at different fixed Ω_2. The center solid line is for Ω_2=0°, to its left is for the counter-propagation configuration, and to its right is for the co-propagation configuration. The straight line is for the co-linear configuration with $\Omega=\Omega_1=\Omega_2$. The point at the origin is the configuration with $\Omega=\Omega_1=\Omega_2=0°$, which is the perpendicular configuration which was used in the CARS imaging studies [29-33].

lower signs correspond to the co-propagation and the counter-propagation configurations, respectively. The general case for nonlinear reflection and transmission was worked out by Bloembergen *et al.* [51]. Of course, here we only discussed the coplanar case because our primary concern is abstract orientational and spectral information for the molecules at the interface or in film. As one knows, the non-coplanar geometry Four-WMS were generally used in the gas phase or liquid phase spectroscopy or dynamics studies, where the major concern was not the orientation and symmetry of the ordered molecular system, but the angular momentum or rotational anisotropy in the random media [52-54].

In the CARS ($\omega=2\omega_1-\omega_2$), there are only three different angles corresponding to each frequency involved, respectively. Eq.(27) defines the possible choices for Ω_1 and Ω_2 if a reflective CARS signal can be observed. Unlike SFG-VS, in which the two incident angles $\Omega_{\rm vis}$ and $\Omega_{\rm IR}$ in the co-propagation or counter-propagation geometry can have almost any values between 0° and 90° from the interface normal, in CARS the choice of Ω_1 and Ω_2 is quite limited. For example, when ω_1=18797 cm^{-1}, i.e. 532 nm, and $\omega_1-\omega_2$=3000 cm^{-1}, the possible Ω_1 and Ω_2 which can generate a real Ω value is between the leftmost and rightmost curves in Fig.3. The center curve is for $\Omega_2 = 0°$. To its right is $\Omega_2>0°$, indicating co-propagation configuration, and to its left is $\Omega_2<0°$, indicating counter-propagation configurations. It is clear here that in CARS not all Ω_1 is accessible once the Ω_2 is fixed, and vise versa.

One particular important case is the co-linear configuration with $\Omega=\Omega_1=\Omega_2$. The perpendicular configuration $\Omega=\Omega_1=\Omega_2=0°$, which is the simplest special case for the co-linear configuration, has been widely employed in CARS imaging studies [29-33]. Another special case for the co-linear configuration is when $\Omega=\Omega_1=\Omega_2=45°$.

Similar to the CARS, the two incident angles in the fourth order CAHRS ($\omega=3\omega_1-\omega_2$) are also similarly constrained. This makes the configuration analysis in CARS and CAHRS quite different from that for the SFG-VS [18,19].

C. The perpendicular and co-linear configuration in the CARS

As a special case for the co-linear configuration, the perpendicular configuration with $\Omega=\Omega_1=\Omega_2=0°$ was generally employed in the CARS imaging studies of molecular films and biological membranes [29-33,55]. In

DOI:10.1088/1674-0068/20/04/449-460

this case, since all the terms with z become zero, there are only two independent polarization measurement for an orientationally isotropic interface or film ($C_{\infty v}$). Following the expressions, we have

$$\begin{aligned}\chi^{(3)}_{\rm eff} &= \cos(\alpha-\alpha_1)\cos(\alpha_1-\alpha_2)\,\chi^{(3)}_{{\rm eff},xxx} \\ &\quad -\sin(\alpha-\alpha_1)\sin(\alpha_1-\alpha_2)\,\chi^{(3)}_{{\rm eff},xyx} \quad (28)\\ \chi^{(3)}_{{\rm eff},xxx} &= \chi^{(3)}_{{\rm eff},yyy} \\ &= \chi^{(3)}_{xxxx}L_{xx}(\omega)\,L^2_{xx}(\omega_1)\,L_{xx}(\omega_2) \quad (29)\\ \chi^{(3)}_{{\rm eff},xyx} &= \chi^{(3)}_{{\rm eff},yxy} \\ &= \chi^{(3)}_{xyyx}L_{xx}(\omega)\,L^2_{yy}(\omega_1)\,L_{xx}(\omega_2) \quad (30)\end{aligned}$$

here the three polarization indexes represent the polarization of the three optical fields of ω, ω_1, and ω_2, respectively. Because the choice of x and y is rather arbitrary, they are exchangeable in all these equations, e.g. $L_{xx}(\omega_i)$=$L_{yy}(\omega_i)$, and $\chi^{(3)}_{{\rm eff},xyx}$=$\chi^{(3)}_{{\rm eff},yxy}$, and $\chi^{(3)}_{{\rm eff},xxx}$=$\chi^{(3)}_{{\rm eff},yyy}$. Generally, in practice we can choose α_1=0°, and Eq.(28) is further simplified into

$$\chi^{(3)}_{\rm eff} = \cos\alpha\cos\alpha_2\chi^{(3)}_{{\rm eff},xxx} + \sin\alpha\sin\alpha_2\chi^{(3)}_{{\rm eff},xyx} \quad (31)$$

In practice, not all ordered films or membranes are rotationally isotropic [30]. The above description gives the criterion to tell whether this is the case from experimental measurement. In the CARS literature, the non-resonant contribution to the CARS signal was also discussed and the polarized CARS (PCARS), as well as other techniques, was employed to differentiate the resonant and non-resonant CARS signal [31,33,55]. In general, considering both the resonant and non-resonant contributions, we have

$$\chi^{(3)}_{ijkl} = \chi^{(3)}_{ijkl,{\rm NR}} + \chi^{(3)}_{ijkl,{\rm R}} \quad (32)$$

The PCARS works when the depolarization ratio $\rho_{\rm NR}$=$\chi^{(3)}_{xyyx,{\rm NR}}/\chi^{(3)}_{xxxx,{\rm NR}}$ is significantly different from the $\rho_{\rm R}$=$\chi^{(3)}_{xyyx,{\rm R}}/\chi^{(3)}_{xxxx,R}$. In practice, in treatment of the PCARS data, $\rho_{\rm NR}$=1/3 is generally used since it was believed that the Kleinman symmetry is generally conserved for the non-resonant processes; while the $\rho_{\rm R}$ is generally different from $\rho_{\rm NR}$, since it has to be somewhere between 0 and 1/3, depending on the symmetry of the vibrational and electronic transitions involved in the CARS process [31,33,55]. Such practice may need some revision, since the Kleinman was proved generally not conserved even very far from the resonance [22,56,57]. The detail of this problem shall be discussed elsewhere.

Experiments with CARS in experimental configuration other than the perpendicular geometry is more complicated. In this case, there are 6 independent experimental terms. The complete expressions of them shall be listed in the supplementary materials for the convenience of future analysis. Obviously there are more information contained in the general CARS measurement. Therefore, the non-perpendicular CARS experiment might provide some unique information which can not be obtained from the perpendicular CARS measurement. However, one has to realize that such experiment can be more difficult to arrange. Furthermore, the detection sensitivity may not be able to be maintained as that for the perpendicular CARS.

The simplest case among the non-perpendicular CARS experiment is with the general co-linear configuration. When the incident angles are tuned, strong configuration and polarization dependence and interference effect in the CARS spectra are expected, as recently demonstrated for the case of SFG-VS [19,20]. Analysis and understanding of these spectra through the change of the general orientational parameters ($c^{(3)}_j$) in the $R_3(\theta)$ in different incident angles should provide abounding information on the molecular spectroscopy and order. The contrast of the CARS image may also be improved in this way.

D. The microscopic $\beta^{(3)}_{i'j'k'l'}$ tensors for the Four-WMS

In the case for crystals, the macroscopic susceptibility tensors are the same as those of the unit cell. So the ensemble average of the microscopic tensors in Eq.(8) is trivial. But for ordered molecular systems, the macroscopic symmetry and the microscopic symmetry are generally not the same, and the ensemble average of the microscopic tensors is complicated. However, in order to employ polarization analysis in nonlinear spectroscopy to study the molecular orientation and its distribution, the detail connection between the macroscopic susceptibility and microscopic (molecular) polarizability tensors need to be known, and only based on this knowledge further simplifications and quantitative calculations of the polarization data become possible, as demonstrated in the recent SHG and SFG-VS studies [9,10,43].

Table I lists the number of independent and non-vanishing experimental observables, the macroscopic susceptibility/microscopic polarizability tensor terms for the third order nonlinear spectroscopy. The detail list of the individual terms are either in the main text or in the supplementary materials for this work.

It is clear in Table I that the number of the independent macroscopic/microscopic tensors are generally larger than the number of independent experimental observables. The total unknown parameters need to be determined in this problem is even larger. It includes the number of independent macroscopic/microscopic tensors, plus two for the orientation angle, and orientational distribution width with the simplest distribution function form such as Gaussian. Therefore, in order to obtain information on the orientation angle, and orientational distribution width, additional quantitative information on the tensorial ratios between the inde-

DOI:10.1088/1674-0068/20/04/449-460

TABLE I The number of independent and non-vanishing terms for the third order nonlinear spectroscopy. Here the results of the general TP-SFG, CARS, and THG are listed.

Name of third-order process	TP-SFG	CRAS	THG
Independent exp. observables for $C_{\infty v}$ interface/film	8	6	4
Total $\chi^{(3)}_{ijkl}/\beta^{(3)}_{i'j'k'l'}$	81	81	81
Non-vanishing $\chi^{(3)}_{ijkl}/\beta^{(3)}_{i'j'k'l'}$ ($C_{\infty v}$)	21	21	21
Independent $\chi^{(3)}_{ijkl}/\beta^{(3)}_{i'j'k'l'}$ ($C_{\infty v}$)	10	10	4
Non-vanishing $\chi^{(3)}_{ijkl}/\beta^{(3)}_{i'j'k'l'}$ (C_{2v})	21	21	21
Independent $\chi^{(3)}_{ijkl}/\beta^{(3)}_{i'j'k'l'}$ (C_{2v})	21	21	9
Non-vanishing $\chi^{(3)}_{ijkl}/\beta^{(3)}_{i'j'k'l'}$ (C_{3v})	41	41	41
$\beta^{(3)}_{i'j'k'l'}$ in $\chi^{(3)}_{ijkl}$ of $C_{\infty v}$ (C_{3v})	21	21	21
Independent $\beta^{(3)}_{i'j'k'l'}$ in $\chi^{(3)}_{ijkl}$ of $C_{\infty v}$ (C_{3v})	10	10	4

pendent $\beta^{(3)}_{i'j'k'l'}$ are needed. In practice, these ratios can either be obtained from theoretical calculation or empirical bond polarizability models based on lower order IR and Raman measurements. Such examples in the SFG-VS studies has been quite successful, and similar approaches may also be applied to the third order CARS or the fourth order CAHRS studies [9,43,58-60].

The non-vanishing and independent $\beta^{(3)}_{i'j'k'l'}$ terms for molecules with $C_{\infty v}$, C_{2v} and C_{3v} symmetries are given below. Here the molecular coordinates are denoted as (a, b, c) with c as the main axis [9].

1. C_{2v} symmetry for the ac plane is defined as the mirror plane

The terms for the general TP-SFG and non-resonant CARS processes are the same. There are 21 non-vanishing terms and they are all independent.

$$\beta^{(3)}_{aacc}, \beta^{(3)}_{acac}, \beta^{(3)}_{ccbb}, \beta^{(3)}_{cbcb}, \beta^{(3)}_{bbcc}, \beta^{(3)}_{bcbc}, \beta^{(3)}_{aabb}, \beta^{(3)}_{abab}, \beta^{(3)}_{bbaa},$$
$$\beta^{(3)}_{baba}, \beta^{(3)}_{ccaa}, \beta^{(3)}_{caca}, \beta^{(3)}_{caac}, \beta^{(3)}_{cbbc}, \beta^{(3)}_{acca}, \beta^{(3)}_{bccb}, \beta^{(3)}_{abba}, \beta^{(3)}_{baab},$$
$$\beta^{(3)}_{aaaa}, \beta^{(3)}_{bbbb}, \beta^{(3)}_{cccc}$$

For resonant CARS process, there are 13 non-vanishing and 7 independent terms for the symmetric stretching (SS) mode, and 8 non-vanishing and 2 independent terms for the asymmetric stretching (AS) mode. For the SS mode:

$$\begin{aligned} A_1 : \beta^{(3)}_{aabb} &= \beta^{(3)}_{bbaa}, \beta^{(3)}_{aacc} = \beta^{(3)}_{ccaa}, \beta^{(3)}_{bbcc} \\ &= \beta^{(3)}_{ccbb}, \beta^{(3)}_{aaaa}, \beta^{(3)}_{bbbb}, \beta^{(3)}_{cccc} \\ A_2 : \beta^{(3)}_{abab} &= \beta^{(3)}_{abba} = \beta^{(3)}_{baab} = \beta^{(3)}_{baba} \end{aligned}$$

and for the AS mode:

$$\begin{aligned} B_1 &: \beta^{(3)}_{acac} = \beta^{(3)}_{acca} = \beta^{(3)}_{caac} = \beta^{(3)}_{caca} \\ B_2 &: \beta^{(3)}_{bcbc} = \beta^{(3)}_{bccb} = \beta^{(3)}_{cbbc} = \beta^{(3)}_{cbcb} \end{aligned}$$

There are 21 non-vanishing and only 9 independent terms for the THG process.

$$\begin{aligned} \beta^{(3)}_{acca} &= \beta^{(3)}_{acac} = \beta^{(3)}_{aacc}, \beta^{(3)}_{cbbc} = \beta^{(3)}_{cbcb} = \beta^{(3)}_{ccbb}, \beta^{(3)}_{bccb} \\ &= \beta^{(3)}_{bcbc} = \beta^{(3)}_{bbcc}, \beta^{(3)}_{cccc} \\ \beta^{(3)}_{aabb} &= \beta^{(3)}_{abab} = \beta^{(3)}_{abba}, \beta^{(3)}_{bbaa} = \beta^{(3)}_{baba} = \beta^{(3)}_{baab}, \beta^{(3)}_{ccaa} \\ &= \beta^{(3)}_{caca} = \beta^{(3)}_{caac}, \beta^{(3)}_{aaaa}, \beta^{(3)}_{bbbb} \end{aligned}$$

2. C_{3v} symmetry for the ac plane is defined as the mirror plane

The C_{3v} terms for the general TP-SFG and non-resonant CARS processes are the same. There are 41 non-vanishing terms, in which 21 terms appear in the $\chi^{(3)}_{ijkl}$ with the $C_{\infty v}$ symmetry, and only 10 terms are independent. The underlined terms are those do not appear in the $\chi^{(3)}_{ijkl}$ with the $C_{\infty v}$ symmetry.

$$\begin{aligned} &\beta^{(3)}_{aaaa} = \beta^{(3)}_{bbbb}, \beta^{(3)}_{cccc} \\ &\beta^{(3)}_{abba} = \beta^{(3)}_{baab}, \beta^{(3)}_{aabb} = \beta^{(3)}_{bbaa}, \beta^{(3)}_{abab} = \beta^{(3)}_{baba} \\ &\beta^{(3)}_{caac} = \beta^{(3)}_{cbbc}, \beta^{(3)}_{ccaa} = \beta^{(3)}_{ccbb}, \beta^{(3)}_{caca} = \beta^{(3)}_{cbcb} \\ &\beta^{(3)}_{acca} = \beta^{(3)}_{bccb}, \beta^{(3)}_{aacc} = \beta^{(3)}_{bbcc}, \beta^{(3)}_{acac} = \beta^{(3)}_{bcbc} \\ &\beta^{(3)}_{accc}, \beta^{(3)}_{ccca}, -\beta^{(3)}_{caaa} = \beta^{(3)}_{cbba} = \beta^{(3)}_{cbab} = \beta^{(3)}_{cabb}, -\beta^{(3)}_{acaa} \\ &\qquad = \beta^{(3)}_{bcba} = \beta^{(3)}_{bcab} = \beta^{(3)}_{acbb} \\ &\beta^{(3)}_{cacc}, \beta^{(3)}_{ccac}, -\beta^{(3)}_{aaca} = \beta^{(3)}_{bbca} = \beta^{(3)}_{bacb} = \beta^{(3)}_{abcb}, -\beta^{(3)}_{aaac} \\ &\qquad = \beta^{(3)}_{bbac} = \beta^{(3)}_{babc} = \beta^{(3)}_{abbc} \end{aligned}$$

and have the connections: $\beta^{(3)}_{aaaa} = \beta^{(3)}_{aabb} + \beta^{(3)}_{abab} + \beta^{(3)}_{abba}$.

For the resonant CARS, for those appear in the $\chi^{(3)}_{ijkl}$ with the $C_{\infty v}$ symmetry, there are 9 non-vanishing and 3 independent terms for the symmetric stretching (SS) mode, and 16 non-vanishing and 2 independent terms

DOI:10.1088/1674-0068/20/04/449-460

for the asymmetric stretching (AS) mode. For the SS mode:

$$\begin{aligned}\beta^{(3)}_{aaaa} &= \beta^{(3)}_{bbbb} = \beta^{(3)}_{aabb} = \beta^{(3)}_{bbaa}, \beta^{(3)}_{aacc} = \beta^{(3)}_{bbcc} = \beta^{(3)}_{ccaa} \\ &= \beta^{(3)}_{ccbb}, \beta^{(3)}_{cccc}\end{aligned}$$

and for the AS mode:

$$\begin{aligned}\beta^{(3)}_{aaaa} &= \beta^{(3)}_{bbbb} = \beta^{(3)}_{abab} = \beta^{(3)}_{baba} = \beta^{(3)}_{abba} = \beta^{(3)}_{baab} \\ &= -\beta^{(3)}_{aabb} = -\beta^{(3)}_{bbaa} \\ \beta^{(3)}_{acac} &= \beta^{(3)}_{bcbc} = \beta^{(3)}_{acca} = \beta^{(3)}_{bccb} = \beta^{(3)}_{caca} = \beta^{(3)}_{cbcb} \\ &= \beta^{(3)}_{caac} = \beta^{(3)}_{cbbc}\end{aligned}$$

For the THG process, there are 41 non-vanishing terms, in which 21 terms appear in the $\chi^{(3)}_{ijkl}$ terms with the $C_{\infty v}$ symmetry, and only 4 terms are independent. The underlined one are those do not appear in the $\chi^{(3)}_{ijkl}$ terms with the $C_{\infty v}$ symmetry.

$$\begin{aligned}&\beta^{(3)}_{cccc}, \beta^{(3)}_{aaaa} = \beta^{(3)}_{bbbb} \\ &\beta^{(3)}_{caac} = \beta^{(3)}_{cbbc} = \beta^{(3)}_{ccaa} = \beta^{(3)}_{ccbb} = \beta^{(3)}_{caca} = \beta^{(3)}_{cbcb} \\ &\beta^{(3)}_{acca} = \beta^{(3)}_{bccb} = \beta^{(3)}_{aacc} = \beta^{(3)}_{bbcc} = \beta^{(3)}_{acac} = \beta^{(3)}_{bcbc} \\ &\beta^{(3)}_{abba} = \beta^{(3)}_{baab} = \beta^{(3)}_{aabb} = \beta^{(3)}_{bbaa} = \beta^{(3)}_{abab} = \beta^{(3)}_{baba} \\ &\beta^{(3)}_{accc}, \beta^{(3)}_{ccca} = \beta^{(3)}_{cacc} = \beta^{(3)}_{ccac}, -\beta^{(3)}_{caaa} = \beta^{(3)}_{cbba} \\ &\qquad = \beta^{(3)}_{cbab} = \beta^{(3)}_{cabb} \\ &-\beta^{(3)}_{acaa} = \beta^{(3)}_{bcba} = \beta^{(3)}_{bcab} = \beta^{(3)}_{acbb} = -\beta^{(3)}_{aaca} = \beta^{(3)}_{bbca} \\ &\qquad = \beta^{(3)}_{bacb} = \beta^{(3)}_{abcb} = -\beta^{(3)}_{aaac} = \beta^{(3)}_{bbac} = \beta^{(3)}_{babc} \\ &\qquad = \beta^{(3)}_{abbc}\end{aligned}$$

and have the connections: $\beta^{(3)}_{aaaa} = 3\beta^{(3)}_{aabb}$.

3. $C_{\infty v}$ symmetry

All terms for the $C_{\infty v}$ symmetry are the same as the terms for the C_{3v} symmetry, except the underlined terms above.

The above terms are the same for the macroscopic $\chi^{(3)}_{ijkl}$ terms with the same macroscopic symmetry. Once the non-vanishing and independent $\beta^{(3)}_{i'j'k'l'}$ terms are known, the expressions for the $\chi^{(3)}_{ijkl}$ terms can be obtained through the ensemble average as described with Eq.(8) and Eq.(9). The detailed expressions for the $\chi^{(3)}_{ijkl}$ terms with $C_{\infty v}$ symmetry for molecules with different symmetry are listed in the supplementary materials. With all these knowledge, one can calculate the general orientational parameters in the $R_3(\theta)$ for polarization and orientational analysis of the experimental data.

IV. THE FOURTH-ORDER NONLINEAR SPECTROSCOPY: FHG AND CAHRS

The general fourth-order nonlinear spectroscopy is usually called the five-wave-mixing spectroscopy (Five-WMS). The general four photon sum frequency generation (FP-SFG) and two typical Five-WMS processes, i.e. FHG and CAHRS, are illustrated in Fig.1(b).

The fourth-order nonlinear spectroscopy is interface specific as the second order SHG and SFG-VS. The possibility for the CAHRS vibrational spectroscopy to overcome the disadvantage of using IR in the SFG-VS is quite promising, despite that the CAHRS process is intrinsically weaker for two or three orders of magnitude that the SFG-VS process [35-39]. Therefore, derivation of the experimental observables and the tensorial relationships for the CAHRS spectroscopy may directly help future applications. It is also helpful for comparison of the CAHRS spectroscopy with the SFG-VS to see what different information can be obtained.

Just like the SFG-VS, the perpendicular experimental configuration in the CAHRS is forbidden for any rotationally symmetric interfaces or films from the interface normal. If any signal is detected from such configuration, the rotational symmetry of the interface or film is broken. This is quite different from the CARS process which has been done mostly in the perpendicular configuration. Therefore, the non-perpendicular co-linear configuration is the simplest configuration one can have in the general CAHRS experiment.

The derivation of the experimental observables and the macroscopic susceptibility/microscopic polarizability tensors for the fourth-order is similar to the above. Here in the main text we only list the number of independent and non-vanishing experimental observables, the macroscopic susceptibility/microscopic polarizability tensor terms for the fourth-order nonlinear spectroscopy. The detail list of the individual terms are given in the supplementary materials for this paper.

V. CONCLUSION

In this paper we presented the description and derivation of the experimental observables and the macroscopic susceptibility/microscopic polarizability tensors for the typical coherent third order and fourth order nonlinear spectroscopy, in the light of applications of these techniques for quantitative polarization and orientational analysis of molecular interfaces, films, and membranes. The complexity of these expressions is by any means daunting for any future applications. This fact also reminds us how much we should have appreciated the relative simplicity in the analysis of the SHG and SFG-VS theories and experiments.

The possibility to further simplify the treatment on the CARS and the CAHRS lies on whether we can have apriori knowledge of the relationship between the

DOI:10.1088/1674-0068/20/04/449-460

TABLE II The number of independent and non-vanishing terms for the fourth order nonlinear spectroscopy. Here the results of the general FP-SFG, CAHRS and FHG are listed.

Name of fourth-order process	FP-SFG	CAHRS	FHG
Independent exp. observables for $C_{\infty v}$ interface/film	16	8	4
Total $\chi^{(4)}_{ijklm}/\beta^{(4)}_{i'j'k'l'm'}$	243	243	243
Non-vanishing $\chi^{(4)}_{ijklm}/\beta^{(4)}_{i'j'k'l'm'}$ ($C_{\infty v}$)	61	61	61
Independent $\chi^{(4)}_{ijklm}/\beta^{(4)}_{i'j'k'l'm'}$ ($C_{\infty v}$)	26	17	5
Non-vanishing $\chi^{(4)}_{ijklm}/\beta^{(4)}_{i'j'k'l'm'}$ (C_{2v})	61	61	61
Independent $\chi^{(4)}_{ijklm}/\beta^{(4)}_{i'j'k'l'm'}$ (C_{2v})	61	41	12
Non-vanishing $\chi^{(4)}_{ijklm}/\beta^{(4)}_{i'j'k'l'm'}$ (C_{3v})	106	106	106
$\beta^{(4)}_{i'j'k'l'm'}$ in $\chi^{(4)}_{ijklm}$ of $C_{\infty v}$ (C_{3v})	61	61	61
Independent $\beta^{(4)}_{i'j'k'l'm'}$ in $\chi^{(4)}_{ijklm}$ of $C_{\infty v}$ (C_{3v})	26	17	5

many macroscopic susceptibility/microscopic polarizability tensors. The development of the field also depends on whether the advancement of the nonlinear spectroscopic experiments can provide novel information about the interface, film and membrane. The experimental studies with various CARS techniques have been quite accessible in many laboratories. To carry out non-perpendicular CARS measurement in different polarizations may help obtain better contrast in the CARS imaging studies. In theory, the application of the CAHRS for probing the vibrational spectroscopy and structure of the buried interfaces is certainly promising. Recent development of the amplification of the very weak photon signals, coherent or incoherent [61-64], indicates that the efficient detection of the very weak coherent CAHRS process without electronic resonance enhancement [35-39] from the molecular interfaces is readily achievable if such amplification techniques can be applied. Thus, the much desired study of the buried liquid/liquid and liquid/solid interfaces with the coherent vibrational spectroscopy can be greatly boosted. Such developments shall make the seemingly tedious efforts in this report worthwhile.

Supplementary Materials. Supplementary materials on the detail expressions for the CARS, THG, CAHRS, and FHG processes are available at the CJCP website alongside the main article.

VI. ACKNOWLEDGMENTS

Yuan Wang thanks the helpful discussions from Wen-kai Zhang, Wei Gan, and De-sheng Zheng. Hong-fei Wang thanks the support by the National Natural Science Foundation of China (No.20373076, No.20425309, No.20533070). Zhi-feng Cui thanks support by the National Natural Science Foundation of China (No.10674002) and the Key Subject of Atomic and Molecular Physics of Anhui Province.

[1] R. H. Tredgold, *Order in Thin Organic Films*, New York: Cambridge University Press, (1994).
[2] G. Roberts, *Langmuir-Blodgett Films*, New York: Kluwar Academic Publishers, (1990).
[3] P. G. de Gennes and J. Prost, *Physics of Liquid Crystal*, 2nd Ed., Oxford: Oxford University Press, (1995).
[4] K. Busch, S. Lölkes, R. B. Wehrspohn, and H. Föll, *Photonic Crystals: Advances in Design, Fabrication, and Characterization*, New York: Wiley-VCH, (2004).
[5] H. F. Wang, Chin. J. Chem. Phys. **17**, 362 (2004).
[6] J. Michl and E. W. Thulstrup, *Spectroscopy with Polarized Light: Solute Alignment by Photoselection, Liquid Crystal, Polymers, and Membranes*, New York: John Wiley & Sons, (1995).
[7] K. B. Eisenthal, Chem. Rev. **96**, 1343 (1996).
[8] Y. R. Shen, Nature **337**, 519 (1989).
[9] H. F. Wang, W. Gan, R. Lu, Y. Rao, and B. H. Wu, Int. Rev. Phys. Chem. **24**, 191 (2005).
[10] W. K. Zhang, H. F. Wang, and D. S. Zheng, Phys. Chem. Chem. Phys. **8**, 4041 (2006).
[11] A. J. Moad and G. J. Simpson, J. Phys. Chem. A **109**, 1316 (2005).
[12] S. H. Lee, J. Wang, S. Krimm, and Z. Chen, J. Phys. Chem. A **110**, 7035 (2006).
[13] C. Hirose, N. Akamatsu, and K. Domen, Appl. Spectr. **46**, 1051 (1992).
[14] Y. Rao, Y. S. Tao, and H. F. Wang, J. Chem. Phys. **119**, 5226 (2003).
[15] R. Lu, W. Gan, B. H. Wu, H. Chen, and H. F. Wang, J. Phys. Chem. B **108**, 7297 (2004).
[16] R. Lu, W. Gan, B. H. Wu, H. Chen, and H. F. Wang, J. Phys. Chem. B **109**, 14118 (2005).
[17] (a) R. Lu, W. Gan, and H. F. Wang, Chin. Sci. Bull. **48**, 2183 (2003).
(b) R. Lu, W. Gan, and H. F. Wang, Chin. Sci. Bull. **49**, 899 (2004).
[18] W. Gan, B. H. Wu, H. Chen, Y. Guo, and H. F. Wang, Chem. Phys. Lett. **406**, 467 (2005).
[19] W. Gan, B. H. Wu, Z. Zhang, Y. Guo, and H. F. Wang, J. Phys. Chem. C**111**, 8716 (2007).
[20] W. Gan, Z. Zhang, R. R. Feng, and H. F. Wang, J. Phys. Chem. C **111**, 8726 (2007).
[21] W. Gan, D. Wu, Z. Zhang, R. R. Feng, and H. F. Wang,

DOI:10.1088/1674-0068/20/04/449-460

J. Chem. Phys. **124**, 114705 (2006).
[22] W. K. Zhang, D. S. Zheng, Y. Y. Xu, H. T. Bian, Y. Guo, and H. F. Wang, J. Chem. Phys. **123**, 224713 (2005).
[23] W. Gan, D. Wu, Z. Zhang, Y. Guo, and H. F. Wang, Chin. J. Chem. Phys. **19**, 20 (2006).
[24] H. Chen, W. Gan, B. H. Wu, D. Wu, Z. Zhang, and H. F. Wang, Chem. Phys. Lett. **408**, 284 (2005).
[25] H. Chen, W. Gan, R. Lu, Y. Guo, and H. F. Wang, J. Phys. Chem. B **109**, 8064 (2005).
[26] H. Chen, W. Gan, B. H. Wu, D. Wu, Y. Guo, and H. F. Wang, J. Phys. Chem. B **109**, 8053 (2005).
[27] A. B. Harvey, *Chemical Applications of Nonlinear Raman Spectroscopy*, New York: Academic Press, (1981).
[28] G. L. Eesley, *Coherent Raman Spectroscopy*, New York: Pergamon Press, (1981).
[29] A. Zumbusch, G. R. Holtom, and X. S. Xie, Phys. Rev. Lett. **82**, 4142 (1999).
[30] J. X. Cheng, S. Pautot, D. A. Weitz, and X. S. Xie, Proc. Natl. Acad. Sci. **100**, 9826 (2003).
[31] J. X. Cheng, L. D. Book, and X. S. Xie, Opt. Lett. **26**, 1341 (2001).
[32] J. X. Cheng and X. S. Xie, J. Phys. Chem. B **108**, 827 (2004).
[33] J. X. Cheng, A. Volkmer, and X. S. Xie, J. Opt. Soc. Am. B **19**, 1363 (2002).
[34] X. L. Nan, A. M. Tonary, A. Stolow, X. S. Xie, and J. P. Pezacki, Chem. Bio. Chem. **7**, 1895 (2006).
[35] S. Fujiyoshi, T. A. Ishibashi, and H. Onishi, J. Phys. Chem. A **108**, 11165 (2004).
[36] S. Fujiyoshi, T. A. Ishibashi, and H. Onishi, J. Phys. Chem. B **108**, 10636 (2004).
[37] S. Fujiyoshi, T. A. Ishibashi, and H. Onishi, J. Phys. Chem. B **109**, 8557 (2005).
[38] S. Fujiyoshi, T. A. Ishibashi, and H. Onishi, J. Phys. Chem. B **110**, 9571 (2006).
[39] S. Yamaguchi and T. Tahara, J. Phys. Chem. B **109**, 24211 (2005).
[40] M. Yang, J. Kim, Y. Jung, and M. Cho, J. Chem. Phys **108**, 4013 (1998).
[41] Minhaeng Cho, J. Chem. Phys. **109**, 2194 (1998).
[42] H. Wu, W. K. Zhang, W. Gan, Z. F. Cui, and H. F. Wang, Chin. J. Chem. Phys. **19**, 187 (2006).
[43] H. Wu, W. K. Zhang, W. Gan, Z. F. Cui, and H. F. Wang, J. Chem. Phys. **125**, 133203 (2006).
[44] G. B. Arfken and H. J. Weber, *Mathematical Methods for Physicists*, 4th Ed., New York: Academic Press, Chapter 12, (1995).
[45] K. Cimatu and S. Baldelli, J. Am. Chem. Soc. **128**, 16016 (2006).
[46] K. Cimatu and S. Baldelli, J. Phys. Chem. B **110**, 1807 (2006).
[47] H. Goldstein, *Classical Mechanics*, Massachusetts: Addison-Wesley Publishing Company, 147, (1980).
[48] Y. R. Shen, *The Principles of Nonlinear Optics*, New York: John Wiley & Sons, (1984).
[49] R. W. Boyd, *Nonlinear Optics*, 2nd Ed., New York: Academic Press, (2002).
[50] A. G. Lambert, P. B. Davies, and D. J. Neivandt, Appl. Spectr. Rev. **40**, 103 (2005).
[51] N. Bloembergen and P. S. Pershen, Phys. Rev. **128**, 606 (1962).
[52] D. M. Jonas, Annu. Rev. Phys. Chem. **54**, 425 (2003).
[53] M. Dantus, Annu. Rev. Phys. Chem. **52**, 639 (2001).
[54] T. A. W. Wasserman, P. H. Vaccaro, and B. R. Johnson, J. Chem. Phys. **108**, 7713 (1998).
[55] A. Y. Chikishev, G. W. Lucassen, N. I. Koroteev, C. Otto, and J. Grevet, Biophys. J. **63**, 976 (1992).
[56] P. A. Franken and J. F. Ward, Rev. Mod. Phys. **35**, 23 (1963).
[57] C. A. Dailey, B. J. Burke, and G. J. Simpson, Chem. Phys. Lett. **390**, 8 (2004).
[58] D. K. Hore, D. K. Beaman, D. H. Parks, and G. L. Richmond, J. Phys. Chem. B **109**, 16846 (2005).
[59] C. Hirose, N. Akamatsu, and K. Domen, J. Chem. Phys. **96**, 997 (1992).
[60] C. Hirose, H. Yamamoto, N. Akamatsu, and K. Domen, J. Phys. Chem. **97**, 10064 (1993).
[61] X. H. Chen, X. F. Han, Y. X. Weng, and J. Y. Zhang, Appl. Phys. Lett. **89**, 061127 (2006).
[62] P. Fita, Y. Stepanenko, and C. Radzewicz, Appl. Phys. Lett. **86**, 021909 (2005).
[63] J. Y. Zhang, A. P. Shreenath, M. Kimmel, E. Zeek, R. Trebino, and S. Link, Opt. Express **11**, 601 (2003).
[64] J. Y. Zhang, C. K. Lee, J. Y. Huang, and C. L. Pan, Opt. Express **12**, 574 (2004).

DOI:10.1088/1674-0068/20/04/449-460